Eur Radiol (2012) 22:2138–2146
DOI 10.1007/s00330-012-2471-9

UROGENITAL

Quantitative elastography of renal transplants using supersonic shear imaging: a pilot study

Nicolas Grenier · Séverine Poulain · Sébastien Lepreux · Jean-Luc Gennisson · Benjamin Dallaudière · Yann Lebras · Eric Bavu · Aude Servais · Vannary Meas-Yedid · Mathieu Piccoli · Thomas Bachelet · Mickaël Tanter · Pierre Merville · Lionel Couzi

Received: 3 January 2012 / Revised: 12 March 2012 / Accepted: 16 March 2012 / Published online: 17 May 2012

Abstract
Purpose To evaluate the reliability of quantitative ultrasonic measurement of renal allograft elasticity using supersonic shear imaging (SSI) and its relationship with parenchymal pathological changes.
Materials and methods Forty-three kidney transplant recipients (22 women, 21 men) (mean age, 51 years; age range, 18–70 years) underwent SSI elastography, followed by biopsy. The quantitative measurements of cortical elasticity were performed by two radiologists and expressed in terms of Young's modulus (kPa). Intra- and inter-observer reproducibility was assessed (Kruskal-Wallis test and Bland-Altman analysis), as well as the correlation between elasticity values and clinical, biological and pathological data (semi-quantitative Banff scoring). Interstitial fibrosis was evaluated semi-quantitatively by the Banff score and measured by quantitative image analysis.
Results Intra- and inter-observer variation coefficients of cortical elasticity were 20 % and 12 %, respectively. Renal cortical stiffness did not correlate with any clinical parameters, any single semi-quantitative Banff score or the level of interstitial fibrosis; however, a significant correlation was observed between cortical stiffness and the total Banff scores of chronic lesions and of all elementary lesions (R=0.34, P=0.05 and R=0.41, P=0.03, respectively).

N. Grenier · B. Dallaudière · Y. Lebras
Service d'Imagerie Diagnostique et Interventionnelle de l'Adulte,
Centre Hospitalier Universitaire de Bordeaux,
Université Bordeaux Segalen,
33076 Bordeaux, France

S. Poulain · T. Bachelet · P. Merville · L. Couzi
Service de Néphrologie et Transplantation Rénale,
Centre Hospitalier Universitaire de Bordeaux,
Université Bordeaux Segalen,
33076 Bordeaux, France

S. Lepreux
Service de Pathologie,
Centre Hospitalier Universitaire de Bordeaux,
Université Bordeaux Segalen,
33076 Bordeaux, France

A. Servais · V. Meas-Yedid · M. Piccoli
Institut Pasteur,
Unité d'Analyse d'Images Quantitative CNRS URA 2582,
25 rue du docteur Roux,
75724 Paris Cedex 15, France

A. Servais
Département de Néphrologie,
Assistance Publique-Hôpitaux de Paris,
Necker-Enfants Malades,
Paris, France

E. Bavu
Laboratoire de Mécanique des Structures et des Systèmes Couplés (EA3196),
Conservatoire National des Arts et Métiers, 292 rue Saint-Martin,
75141 Paris Cedex 03, France

J.-L. Gennisson · M. Tanter
Institut Langevin—Ondes et Images, ESPCI Paris Tech,
CNRS UMR 7587,
INSERM ERL U979, 10 rue Vauquelin,
75231 Paris Cedex 05, France

N. Grenier (✉)
CHU Bordeaux—Groupe Hospitalier Pellegrin,
Service de Radiologie, Place Amélie Raba Léon,
33076 Bordeaux, France
e-mail: nicolas.grenier@chu-bordeaux.fr

Conclusion Quantitative measurement of renal cortical stiffness using SSI is a promising non-invasive tool to evaluate global histological deterioration.

Key Points

- *Supersonic shear imaging elastography can measure cortical stiffness in renal transplants*
- *The level of cortical stiffness is correlated with the global degree of tissue lesions*
- *The global histological deterioration of transplanted kidneys can be quantified using elastography*

Keywords Kidney · Transplantation · Elastography · Ultrasound · Renal fibrosis

Introduction

The development of interstitial fibrosis and tubular atrophy (IF/TA), previously called chronic allograft nephropathy (CAN) [1], is the major determinant of renal allograft failure after kidney transplantation. The natural history of IF/TA in transplanted kidneys has been well studied through protocol biopsies. The early phase, which generally occurs during the first years post-transplantation, is characterised by fibrogenesis and the emergence of tubulointerstitial damage due to immunological phenomena; the late phase is characterised by the worsening of parenchymal lesions (irreversible interstitial fibrosis, tubular atrophy, arteriolar hyalinosis) and the occurrence of glomerular sclerosis, leading to graft loss [2, 3].

Non-invasive markers of these pathological changes are lacking and protocol biopsies are still the only reliable tool for the diagnosis of IF/TA. The increase in creatininaemia is detected at a later stage when lesions are irreversible and thus is not adequate for following the early progression of IF/TA. Transplant biopsy remains an invasive approach and is associated with possible haematuria, haematomas, arteriovenous fistula and, in rare cases, transplant loss despite ultrasound guidance. Therefore, there is a critical need to develop non-invasive and reproducible alternatives. Quantitative elastography is now a well-established method for screening and monitoring liver tissue stiffness. Conversely, static elastography is not adequate for that purpose because it is not quantitative [4]. Quantitative transient elastography (Fibroscan®, Echosens, Paris) has been validated for screening and monitoring liver fibrosis in chronic hepatitis, permitting many patients to avoid biopsy [5–7]. Acoustic radiation force impulse (ARFI) (Acuson S2000; Siemens Medical Solutions, Mountain View, CA, USA) is another promising quantitative transient elastography technique for assessing liver fibrosis [8]. Both of these techniques are unidimensional and were recently evaluated in kidney transplants in three pilot studies [9–11] with contradictory results and without systematic evaluation of all pathological items. The quantitative bidimensional supersonic shear imaging (SSI) technique was successfully implemented on curved arrays for in vivo liver elasticity mapping [12]. Recently, its ability to assess the degree of liver fibrosis of hepatitis C patients was also investigated in 113 patients with very promising results [13]. For all these reasons, we conducted a pilot study using the SSI technique in transplanted kidneys in order to evaluate the intra- and inter-observer reproducibility of cortical stiffness measurement and its potential correlation with all histological lesions described in the Banff classification [1, 14].

Materials and methods

Subjects

Between January 2010 and May 2010, 49 consecutive kidney transplant recipients (KTRs) scheduled for renal biopsy at the Bordeaux Hospital were included in this study (47 deceased donors and two living donors) to perform both transplant biopsy and transplant stiffness measurement using SSI. Nine of the patients were transplanted with anti-donor-specific antibodies and thus had a protocol biopsy during the first 3 months post-transplantation. All other patients had a clinically indicated biopsy: nine during the first year post-transplantation and 31 after the first year post-transplantation. This prospective study was approved by the French National Committee for the Protection of Patients Participating in Biomedical Research Programs ("CPP du Sud-Ouest et Outre Mer III", 2008-A00834-51), and all patients provided written informed consent.

Elastography sequence and data processing

Measurements of renal stiffness were performed just before biopsy by two radiologists (N.G. and B.D.) who were blinded to each other's results. Eight successive measurements in the cortex and in the medulla were performed in each patient by each radiologist. An ultrafast ultrasound device (Aixplorer®, SuperSonic Imagine, Aix-en-Provence, France) was used with a 3.5 MHz probe (SC6-1, SuperSonic Imagine). The principles of SSI have been previously reported [15, 16]. Briefly, a vibration force was generated in tissues by four successive ultrasound beams focused at different depths (5-mm spacing). Each focused beam, a so-called pushing beam, consisted of a 150-μs burst at 8 MHz. Propagating shear waves were imaged at a very high frame rate (up to 20,000 frames/s) and raw radiofrequency data were recorded. The movies of displacements induced in tissues by the shear wave were calculated using the speckle tracking correlation technique. Then the shear wave speed (c_T) was locally deduced by applying a

time-of-flight algorithm to these movies. The elastic modulus, the so-called Young's modulus (E), was calculated from the shear wave speed in locally homogeneous soft tissues based on the following equation: $1E \approx 3\mu = 3\rho c_T^2$, where μ is the shear modulus and ρ is the density. Results were displayed on a colour scale in kPa (Young's modulus) as presented in Fig. 1.

The colour scale elasticity map was positioned to cover the anterior aspect of the lower pole of the transplant, corresponding to the biopsy site. Data analysis of elasticity values was performed by using regions of interest within the cortex and the medulla. The regions of interest were approximately 1 cm^2 and drawn by each observer within the cortex and within the medulla. Measurements with a standard deviation value greater than 30 % of the mean within the region of interest were considered as inadequate and were subsequently excluded from data analysis.

Biopsy

Cortical biopsies were performed in the lower pole of the graft with a 16 gauge biopsy needle guided by ultrasound. For histological examination by light microscopy, biopsy specimens were fixed, embedded in paraffin, sectioned at 2 μm, and stained with Masson's trichrome, haematoxylin-eosin and periodic acid Schiff. Histological analyses were performed by one pathologist (S.L.) who was blinded to the elastography results. All biopsies were graded according to the updated semi-quantitative Banff classification [1, 14] by scoring each of the following parameters: interstitial inflammation (i), tubulitis (t), glomerulitis (g), intimal arteritis (v), peritubular capillaritis (cpt), interstitial fibrosis (ci), tubular atrophy (ct), allograft glomerulopathy (cg), mesangial matrix increase (mm), fibrous intimal thickening (cv), arteriolar hyaline thickening (ah). A scoring of IF/TA was also calculated by adding up the ci and ct scores.

Interstitial fibrosis measurement by quantitative image analysis

For all biopsies, a cortical section stained with green trichrome was centrally imaged in a blinded manner using a Zeiss Mirax Scan slide device with a 20× objective (NA=0.8) and a CCD Marlin camera. As this set-up is a virtual microscope, we chose one resolution for image processing and thus exported the images to tiff format at a scale of 1:8. For each biopsy, a cortical section from one slide was captured. The medulla was eliminated at the acquisition phase or during analysis by the observer. For each biopsy, the entire cortical region was analysed in a stepwise fashion as a series of consecutive fields. Images were analysed by new colour segmentation image analysis software (Patent EU number 2004292513–1). We used clustering techniques to reduce the colour image into three colour classes, in the I1H2H3 colour space defined by I1 = (R + G + B)/3, H2 = R - G and H3 = (R + G)/2 - B. Then, two masks were extracted from the reduced colour image: (1) the cortical biopsy area and (2) the green mask. The interstitial fibrosis area is defined as the surface of green pixel minus the pixels of

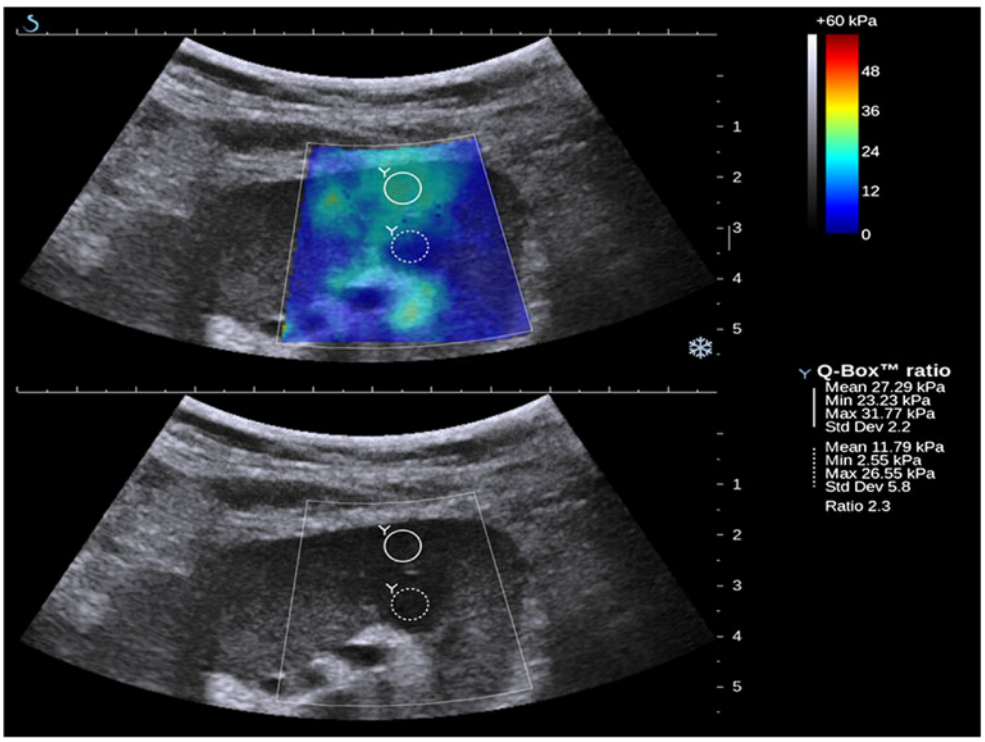

Fig. 1 Example of quantitative elasticity map of the lower pole of a kidney transplant. The regions of interest are positioned in the cortex (*open circle*) and the medulla (*dashed circle*) using the B-mode image. The colour map is a distribution of elasticity values scaled from 0 to 60 kPa and calculated from shear wave velocity values using Young's modulus

tubular basement membranes, capsule, glomeruli and vessels. The index of the interstitial fibrosis is defined as the ratio between the interstitial fibrosis area and the total surface of the cortex area in the biopsy. The segmentation procedure is sufficiently robust for the various degradation factors that can affect image quality, such as histological section quality and colour staining. The inter- and intra-observer standard deviations for quantitative image analysis were 0.88 (95 % CI: 0.68–0.99, P=7.5e-12) and 0.90 (0.63–0.99, P=3.54e-13), respectively [17, 18].

Statistical analysis

Mean cortical and mean medullary elasticity values were calculated for each patient. Intra- and inter-observer reproducibility were assessed by a coefficient of variation (CV = SD/mean × 100) and agreement was assessed by an intra-class correlation coefficient. Reproducibility analysis between the two observers was also performed using the Kruskal–Wallis test and the Bland–Altman test. Because stiffness values were not normally distributed, the median of the eight measurements obtained in each patient was calculated and used for subsequent analysis. Pearson's correlation analysis was used to measure the correlations between kidney stiffness and the clinical parameters and the Banff semi-quantitative scores. Analyses were performed with Statview Software (Abacus Concepts, Berkeley, CA, USA).

Results

The assessment of renal allograft parenchymal stiffness was successful in 43 patients. The characteristics of these 43 KTR with SSI quantitative elastography and transplant biopsy data are summarised in Table 1.

Renal pathological conditions

The mean number of glomeruli per biopsy was 11.6±6.6. The diagnoses made by the pathologist were: IF/TA (n=31), BK virus nephropathy (n=2), chronic active antibody-mediated rejection (n=7), acute antibody-mediated rejection (n=1), acute T-cell-mediated rejection (n=1) and acute tubular necrosis (n=1). The semi-quantitative scoring of renal lesions showed mainly tubular atrophy and interstitial fibrosis lesions (Table 2). The mean percentage of interstitial fibrosis measured by quantitative image analysis across all patients was 32.4±10.8 %. We observed a very good correlation between the measurements of interstitial fibrosis by the semi-quantitative Banff score and the quantitative image analysis (r=0.74, P=0.0001). C4d deposition was only found in one patient. The patient displaying acute tubular necrosis was excluded from the subsequent analysis because the t score was not applicable.

Table 1 Patients' characteristics

Donor		Value
Age (years)		50 [17–75]
Expanded criteria donor (%)		15 (35 %)
Hypertension (%)		9 (21 %)
Cerebral stroke (%)		16 (37 %)
Cardiac arrest (%)		9 (21 %)
Creatininaemia (μmol/l)		80 [38–404]
Ischaemia (hours)		18 [1–38]
Number of HLA mismatches		2 [0–5]
Recipient		
Age (years)		51 [18.5–69.9]
Sex (men, %)		21 (49 %)
Weight (kg)		71 [40–92]
Height (cm)		168 [148–185]
Body mass index (kg/m²)		25 [17.8–32.0]
Sensitised patients (%)		18 (42 %)
Creatininaemia at biopsy (μmol/l)		174 [65–437]
Estimated glomerular filtration rate (MDRD, ml/min)		34 [12–83]
Proteinuria (g/l)		0.3 [0–5.6]
Time between transplantation and biopsy (months)		26.6 [0.3–214.3]
Delayed graft function (%)		11 (26 %)
Past medical history of acute rejection (%)		4 (9 %)
Cytomegalovirus infection (%)		12 (28 %)
Induction treatment (%)		
	No/Simulect/ Thymoglobulin	3 (7 %) / 22 (51 %) / 18 (42 %)
Treatment at biopsy (%)		
	Tacrolimus/ Cyclosporine/ Everolimus	31 (72 %) / 10 (23 %) / 2 (5 %)
	Mycophenolate mofetil/Imurel	40 (93 %) / 2 (5 %)
	Steroids	28 (65 %)
Initial nephropathy (%)		
	Glomerular	18 (42 %)
	Hereditary	9 (21 %)
	Tubulo-interstitial	7 (16 %)
	Hypertensive	4 (9 %)
	Undetermined	5 (12 %)

Unless otherwise stated, results are given as median (min – max) or n (%)

HLA human leucocyte antigen, *MDRD* modification of diet in renal disease

Table 2 Correlation between histological Banff scores and renal stiffness by elastography

	Mean ± SD	*r*	*P* value
Banff semi-quantitative score			
i	0.6±0.7	0.279	0.09
t	0.1±0.5	0.118	0.5
g	0	-	-
v	0	-	-
cpt	0.16±0.4	0.291	0.08
ci	1.5±0.8	0.286	0.09
ct	1.4±0.9	0.261	0.1
cg	0.5±0.9	0.164	0.3
mm	± 0.3	0.259	0.1
cv	0.9 ±0.9	0.255	0.1
ah	0.9±0.8	0.089	0.6
Percentage of glomerular sclerosis	20.1±24.6	0.084	0.6
Sum of Banff score			
i + t + v	0.6±1.0	0.313	0.08
g + v + cpt	0.2±0.5	0.261	0.1
ci + ct	3.0±1.6	0.277	0.1
ci + ct + cg + cv	4.4±2.5	0.342	0.05
i + t + g + v + cpt + ci + ct + cg + mm + cv + ah	6.0±3.6	0.410	0.03

Interstitial inflammation (*i*), tubulitis (*t*), glomerulitis (*g*), intimal arteritis (*v*), peritubular capillaritis (*cpt*), interstitial fibrosis (*ci*), tubular atrophy (*ct*), allograft glomerulopathy (*cg*), mesangial matrix increase (*mm*), fibrous intimal thickening (*cv*), arteriolar hyaline thickening (*ah*)

Measurement of renal allograft stiffness by elastography

The mean number of adequate measurements per patient was 7.9±0.3 in the cortex and 7.2±1.4 in the medulla for the first observer and 7.6±1.0 in the cortex and 6.7±1.8 in the medulla for the second observer (Table 3). The intra-observer variability coefficients were 20 % and 22 % in the cortex and 32 % and 31 % in the medulla for the first and second observers, respectively. The median stiffness values obtained by the two observers were 22.9±2.7 kPa in the cortex and 16±2.9 kPa in the medulla. The inter-observer variability coefficients were 12 % in the cortex and 18 % in the medulla. Inter-observer agreement was greater for the cortex than the medulla with intra-class correlation coefficients of 0.60 (0.34–0.76, $P=3.15\times10^{-5}$) and 0.26 (−0.07 to 0.54, $P=6.14\times10^{-2}$), respectively. This was confirmed by the Kruskal–Wallis and the Bland–Altman tests (Fig. 2). In three KTR, we observed a large discrepancy in cortical stiffness measurement, characterised by inter-observer variability higher than 30 %. These patients were excluded from the subsequent correlation analyses.

Table 3 Measurement of renal allograft stiffness by elastography

	Cortex	Medulla
Observer 1		
Number of measurement	7.9±0.3	7.2±1.4
Median stiffness (kPa)	23.6 [8.8−41.2]	17.5 [9.1−28.8]
Variability coefficient (%)	20	32
Observer 2		
Number of measurement	7.6±1.0	6.7±1.8
Median stiffness (kPa)	22.5 [12.7−49.4]	15.5 [9.5−43.0]
Variability coefficient (%)	22	31
Observers 1 and 2		
Median value (kPa)	22.9 [11.7−42.6]	16 [10.6−32.0]
Variability coefficient (%)	12	18

Unless otherwise stated, values are given as mean ± SD or median [min – max]

Correlations between cortical stiffness and clinical and biological parameters

For the remaining 39 patients, the mean of the median stiffness values measured by the two observers for each patient was compared with clinical, biological and pathological data. We did not observe any correlation between renal cortical stiffness and donor characteristics (age, extended criteria donor, history of cardiac arrest, history of hypertension, serum creatinine), recipient characteristics at the time of biopsy (age, sex, time between transplantation and biopsy, weight, height, body mass index, estimated glomerular filtration rate by MDRD formula, proteinuria, type of immunosuppressive treatment), number of HLA mismatches, total duration of ischaemia, history of delayed graft function, history of acute rejection or history of CMV infection.

Correlations between cortical stiffness and pathological condition

Correlations between renal cortical stiffness and each individual score of the semi-quantitative Banff classification are detailed in Table 2. None of these scores was correlated with the measurement of cortical stiffness, including interstitial fibrosis (ci) (Fig. 3a). Moreover, cortical stiffness was correlated with neither the level of interstitial fibrosis measured by quantitative image analysis (Fig. 3b) nor the scoring and grading of IF/TA (ci + ct) (Fig. 3c, d, respectively). Interestingly, renal cortical stiffness did correlate with the sum of the scores of chronic lesions (ci + ct + cg + cv) and the sum of the scores of all individual lesions (i + t + g + v + cpt + ci + ct + cg + mm + cv + ah) (R = 0.34, P=0.05 and R = 0.41, P=0.03, respectively; Fig. 3e, f).

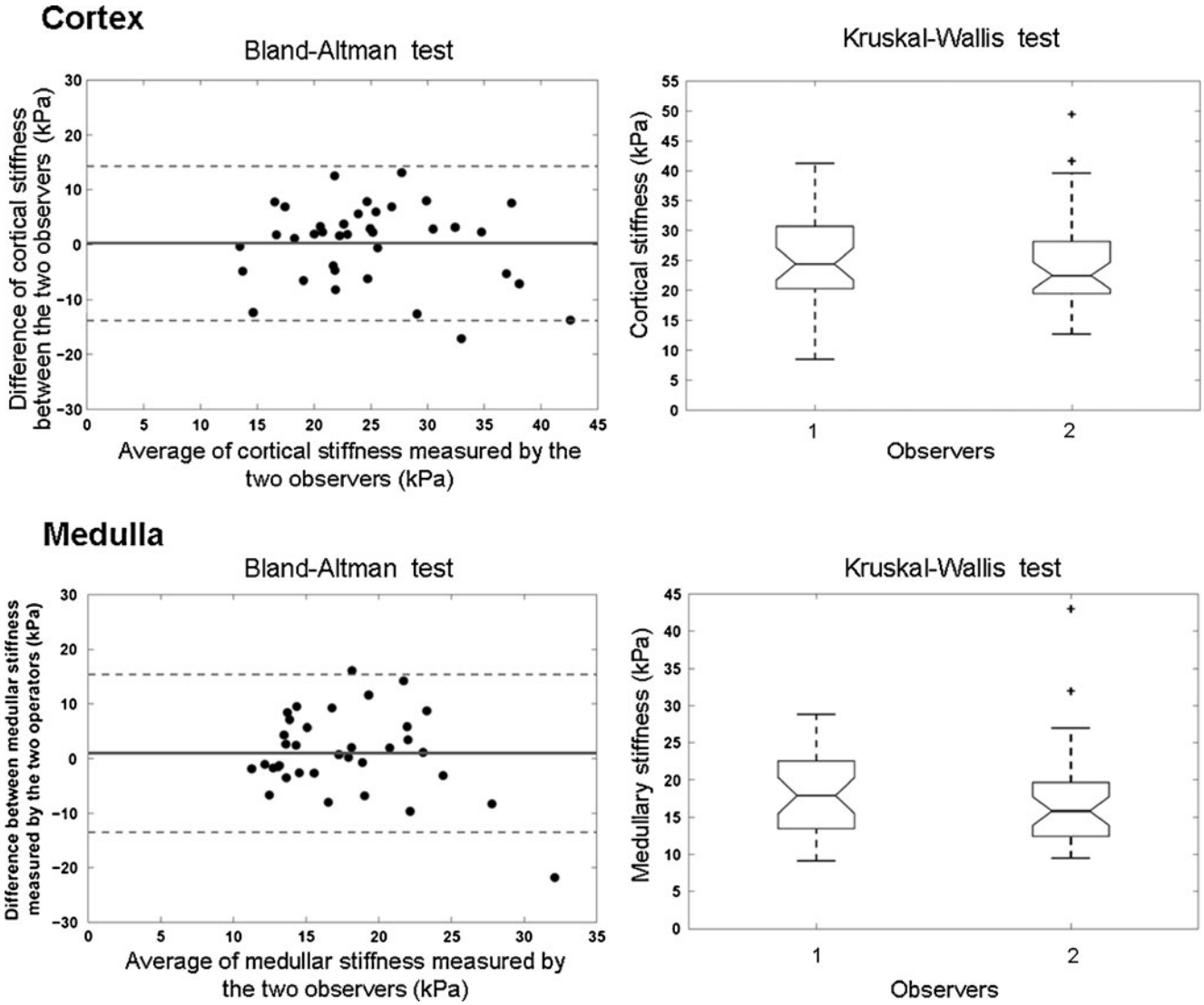

Fig. 2 Inter-observer reproducibility evaluated by Bland–Altman plots and the Kruskal–Wallis test. The Bland-Altman plot compares independent measurements of cortical and medullary stiffness of two observers in 43 transplanted kidneys. For each observer and each patient, stiffness values are median values calculated from eight individual measurements. The difference between the two observers is expressed as a percentage deviation from the average of both observers. Horizontal lines are drawn at the mean difference and at the mean difference plus and minus 1.96-times the standard deviation of differences

Discussion

This study shows that transplanted kidney cortical stiffness measurement using the non-invasive SSI technique is feasible and reproducible. This stiffness measurement reflects a global histological deterioration characterised by the sum of each individual pathological lesion described in the Banff classification.

Our cohort can be considered representative of the kidney transplant population in terms of patients' age, sex, deceased or living donor, immunosuppressive treatment, and acute rejection incidence. In order to have a heterogeneous and representative population, we included patients who had either a protocol biopsy or a clinically indicated biopsy. In this latter group, we included both KTR with a follow-up within and after 1 year post-transplantation, in order to have various histological lesions. As expected, histological analysis showed a high IF/TA incidence, which is the predominant pathological change observed in transplanted kidney [19].

The feasibility of renal sampling using SSI reaches 88 %. Reliable data could not be obtained in 12 % (six patients). Of these, 6 % were due to sampling failures (three patients) with inadequate elasticity maps showing incomplete data filling. This could be due to a lack of sensitivity of the system according to the quality of transmission of the acoustic "pushing" beam responsible for an inadequate signal/noise ratio. The other 6 % were due to more than 50 % of inadequate

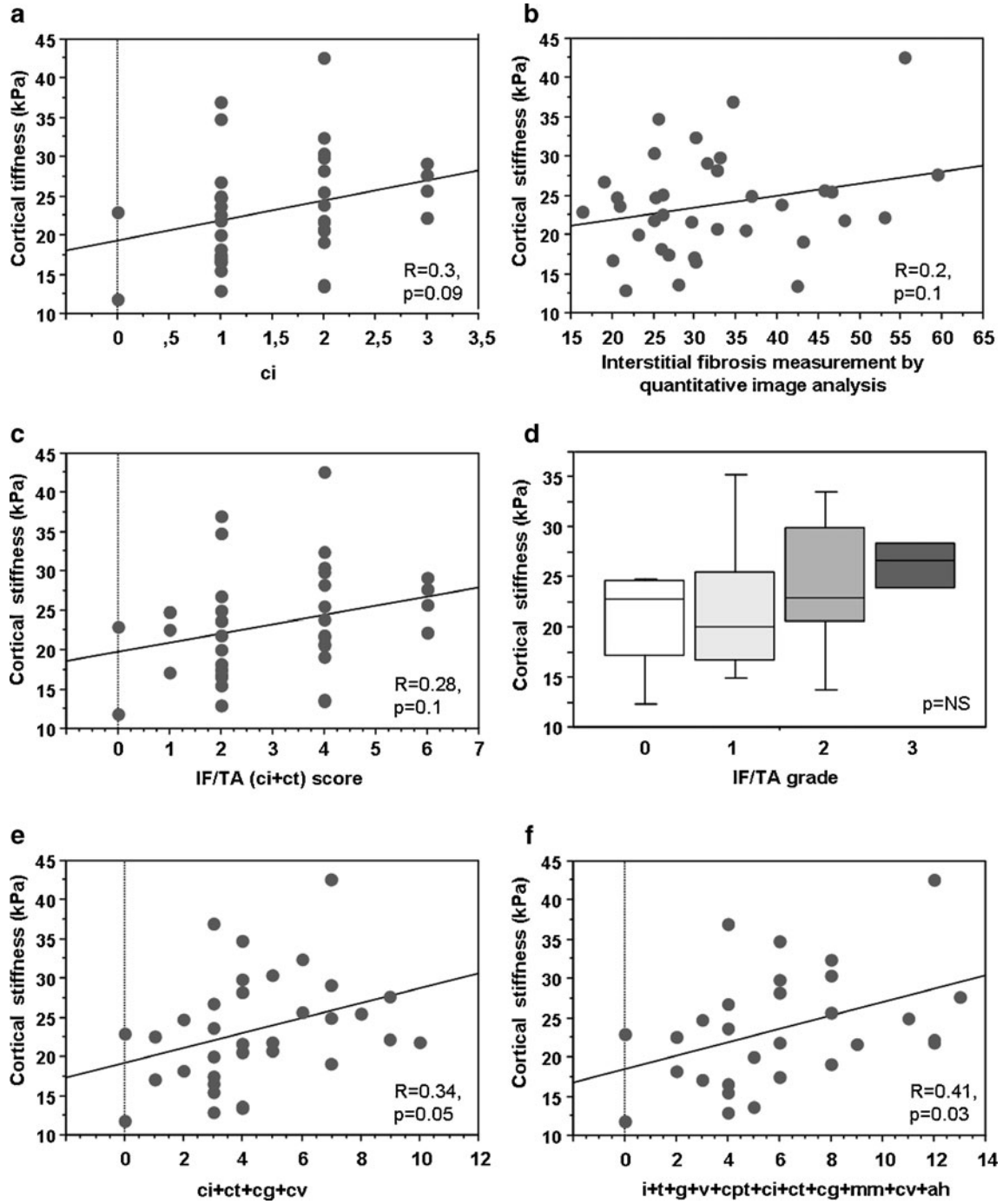

Fig. 3 The relationships between cortical stiffness and semi-quantitative scoring of interstitial fibrosis (**a**), quantitative measurement of interstitial fibrosis by image analysis (**b**), IF/TA scoring (**c**) and grading (**d**), sum of individual chronic changes (**e**) and sum of all pathological changes (**f**). Interstitial inflammation (*i*), tubulitis (*t*), glomerulitis (*g*), intimal arteritis (*v*), peritubular capillaritis (*cpt*), interstitial fibrosis (*ci*), tubular atrophy (*ct*), allograft glomerulopathy (*cg*), mesangial matrix increase (*mm*), fibrous intimal thickening (*cv*), arteriolar hyaline thickening (*ah*)

measures. This failure rate is higher than those reported in the liver with the Fibroscan® (2.4–9.4 % failure rates) [20], mainly related to obesity [5]. This difference between the two organs may be explained by the difference in the depth of the sampling zone and by the interposition of post-operative heterogeneous tissue between the probe and the graft after renal transplantation.

The intra-observer variability coefficients were considered acceptable for the cortex (20 % and 22 %) but unacceptable for the medulla (31 % and 32 %). A similar level of intra-observer

variability was reported for renal cortex using the ARFI system (i.e. between 22 and 24 %) [10]. In the liver, the intra-observer variability is much lower than that reported in the kidney, with coefficients of variation < 5 % using Fibroscan® [20] and 3.9 % using SSI [12]. To our knowledge, ARFI has not been analysed for intra-observer variability in the liver [8].

These results highlight the difference between these two organs with respect to reproducibility, the liver tissue being much more homogeneous than the renal tissue. This variability could be explained by several parameters: (1) unlike the liver, the kidney is characterised by a complex anatomical organisation with several compartments; (2) the large differences in blood flow between the kidney (a high-pressure arterial flow) and the liver (mainly a low-pressure venous flow); (3) the cellular architecture in kidney is highly anisotropic, as has been shown with diffusion-weighted magnetic resonance imaging [21], which may have a serious impact on shear wave onset (the efficiency of the acoustic push in creating a shear wave depends on the orientation of the tissue interfaces) and propagation (shear wave propagation velocity is dependent on tissue orientation, being higher in the direction of the main tissue directivity).

Similarly, inter-observer variability and intra-class correlation coefficients were acceptable for the cortex. There was no correlation between this variability and weight, height, body mass index (BMI) or any other factor related to the patient (data not shown). A good inter-observer agreement was also reported using ARFI [10]. We have no explanation for the high inter-observer variability coefficient (>30 %) obtained in three patients and these values have been excluded from the subsequent correlation analysis.

The correlation between renal elasticity quantification and intra-renal pathological changes is quite controversial in the literature. Arndt et al. [9], using the Fibroscan®, found a correlation between renal stiffness and the degree of interstitial fibrosis, whereas Syversveen et al [10], using ARFI, did not. Conversely, Stock et al. [11] found a positive but moderate correlation between mean ARFI values and the grade of fibrosis, based on 18 patients only. The positive correlation reported with Fibroscan® is quite surprising because this system drives a fixed sampling volume in depth and it is not image-guided, which is a major limitation considering the compartmentalisation of the kidney. In the present study, quantitative two-dimensional (2D) mapping of renal stiffness shows no correlation with interstitial fibrosis by using either the classical semi-quantitative Banff score or the quantitative image analysis. One possible explanation for this discrepancy is the non-specificity of stiffness changes related to interstitial fibrosis. This is confirmed by the correlation we obtained between cortical stiffness and the sum of all semi-quantitative Banff lesions. However, comparative studies between SSI and ARFI would be worthwhile in the future.

In summary, our results suggest that the degree of renal cortical stiffness does not reflect any specific intra-renal change, such as fibrosis, but rather the association of several renal microlesions, especially chronic lesions. This study also suggests that the quantification of tissue stiffness using ultrasound is more complex within the kidney than within the liver because of high tissue heterogeneities and anisotropy, increasing its variability. Before conducting any additional studies, it will be necessary to evaluate more precisely the effect of anisotropy on elasticity values within each renal compartment and probably the role of urinary pressure and tissue perfusion in this highly vascularised organ.

Acknowledgements We thank Catherine Rio for her help as a nurse coordinator. We thank Jean-Christophe Olivo-Marin, Régis Hubrecht and Eric Thervet for their contribution to this study.

Conflicts of interest N.G. is a member of the scientific advisory board of SuperSonic Imagine, J.L.G. is a consultant for SuperSonic Imagine, and M.T. is cofounder and a shareholder of SuperSonic Imagine (Aix-en-Provence, France). J.L.G. and M.T. provided the equipment and technical support (programming of ultrasound sequences and data post-processing). Data were controlled by two of the authors (L.C. and N.G.) who do not have any financial interest. R.H., Y.L., S.P., T.B., P.M., L.C., S.L., A.S., V.M.Y., M.P. and E.B. have no conflicting financial interests. There was no study sponsor.

References

1. Racusen LC, Solez K, Colvin RB et al (1999) The Banff 97 working classification of renal allograft pathology. Kidney Int 55:713–723
2. Nankivell BJ, Borrows RJ, Fung CL, O'Connell PJ, Allen RD, Chapman JR (2003) The natural history of chronic allograft nephropathy. N Engl J Med 349:2326–2333
3. Stegall MD, Park WD, Larson TS et al (2010) The histology of solitary renal allografts at 1 and 5 years after transplantation. Am J Transplant 11:698–707
4. Weitzel WF, Kim K, Rubin JM et al (2004) Feasibility of applying ultrasound strain imaging to detect renal transplant chronic allograft nephropathy. Kidney Int 65:733–736
5. de Ledinghen V, Vergniol J (2008) Transient elastography (FibroScan). Gastroenterol Clin Biol 32:58–67
6. Nguyen-Khac E, Capron D (2006) Noninvasive diagnosis of liver fibrosis by ultrasonic transient elastography (Fibroscan). Eur J Gastroenterol Hepatol 18:1321–1325
7. Sandrin L, Fourquet B, Hasquenoph JM et al (2003) Transient elastography: a new noninvasive method for assessment of hepatic fibrosis. Ultrasound Med Biol 29:1705–1713
8. Friedrich-Rust M, Wunder K, Kriener S et al (2009) Liver fibrosis in viral hepatitis: noninvasive assessment with acoustic radiation force impulse imaging versus transient elastography. Radiology 252:595–604
9. Arndt R, Schmidt S, Loddenkemper C et al (2010) Noninvasive evaluation of renal allograft fibrosis by transient elastography – a pilot study. Transpl Int 23:871–877
10. Syversveen T, Brabrand K, Midtvedt K et al (2010) Assessment of renal allograft fibrosis by acoustic radiation force impulse quantification – a pilot study. Transpl Int 24:100–105

11. Stock KF, Klein BS, Vo Cong MT et al (2010) ARFI-based tissue elasticity quantification in comparison to histology for the diagnosis of renal transplant fibrosis. Clin Hemorheol Microcirc 46:139–148
12. Muller M, Gennisson JL, Deffieux T, Tanter M, Fink M (2009) Quantitative viscoelasticity mapping of human liver using supersonic shear imaging: preliminary *in vivo* feasibility study. Ultrasound Med Biol 35:219–229
13. Bavu E, Gennisson JL, Couade M et al (2011) Noninvasive *in vivo* liver fibrosis evaluation using supersonic shear imaging: a clinical study on 113 hepatitis C virus patients. Ultrasound Med Biol 37:1361–1373
14. Sis B, Mengel M, Haas M et al (2010) Banff '09 meeting report: antibody mediated graft deterioration and implementation of Banff working groups. Am J Transplant 10:464–471
15. Athanasiou A, Tardivon A, Tanter M et al (2010) Breast lesions: quantitative elastography with supersonic shear imaging – preliminary results. Radiology 256:297–303
16. Bercoff J, Tanter M, Fink M (2004) Supersonic shear imaging: a new technique for soft tissue elasticity mapping. IEEE Trans Ultrason Ferroelectr Freq Control 51:396–409
17. Servais A, Meas-Yedid V, Buchler M et al (2007) Quantification of interstitial fibrosis by image analysis on routine renal biopsy in patients receiving cyclosporine. Transplantation 84:1595–1601
18. Servais A, Meas-Yedid V, Toupance O et al (2009) Interstitial fibrosis quantification in renal transplant recipients randomized to continue cyclosporine or convert to sirolimus. Am J Transplant 9:2552–2560
19. Matas AJ, Gillingham KJ, Humar A et al (2008) 2202 kidney transplant recipients with 10 years of graft function: what happens next? Am J Transplant 8:2410–2419
20. Castera L, Bernard PH, Le Bail B et al (2011) Transient elastography and biomarkers for liver fibrosis assessment and follow-up of inactive hepatitis B carriers. Aliment Pharmacol Ther 33:455–465
21. Ries M, Jones RA, Basseau F, Moonen CT, Grenier N (2001) Diffusion tensor MRI of the human kidney. J Magn Reson Imaging 14:42–49